DSMO Sensorless Control of BLDCM Based on Exponential Approach Law

Fan Qigao[1],Sunyan [2] , Wuyaheng [3]and Sunbiwen [4]

[1] Key Laboratory of Advanced Process Control for Light Industry, Jiangnan University, Wuxi, Jiangsu Province, 214122, China

[2] Key Laboratory of Advanced Process Control for Light Industry, Jiangnan University, Wuxi, Jiangsu Province, 214122, China

[3] Key Laboratory of Advanced Process Control for Light Industry, Jiangnan University, Wuxi, Jiangsu Province, 214122, China

[4]Key Laboratory of Advanced Process Control for Light Industry, Jiangnan University, Wuxi, Jiangsu Province, 214122, China

Abstract

The brushless DC motor (BLDCM) is a multi-variable nonlinear control system with strong coupling, which is designed to overcome limitations of the continuous domain control method. Discrete-time sliding mode observer (DSMO) sensorless control of the BLDCM is proposed based on the exponential approach law. The Sigmoid function is used to weaken the chattering problem, and an electromotive force observer is built to extract the electromotive force signal directly. Lyapunov theory is also used to prove the stability of the algorithm. In order to estimate the position and speed of the rotor accurately, a Coordinate Rotation Digital Computer (CORDIC) algorithm is introduced. Experimental results demonstrate that the control strategy can accurately estimate the position and speed of the rotor weaken the chattering problem of the observer and improve the system precision and reliability.

1 Introduction

The brushless DC motor (BLDCM) is widely used in different fields due to its simple structure and high power density [1] . A BLDCM system that is sensorless also saves space as it does not require installation of sensors and efficiently improves the system reliability and efficiency. A sensorless control strategy has become a hot research topic in the brushless DC motor field.

The rotor position detection directly affects the stability and precision of the BLDM control system; so many researchers have proposed different detection methods. Zou [2] described a switched-capacitor filter which creates a fixed phase delay, with a lag-in phase that is independent of the speed of the rotor. Since the phase has a constant delay of 90°, when the motor speed is changed, a rotor position signal that does not require phase compensation is obtained, however the hardware circuit is very complex. Y.Inoue [3] used an online parameter identification method

IJCSI International Journal of Computer Science Issues, Volume 12, Issue 6, November 2015
ISSN (Print): 1694-0814 | ISSN (Online): 1694-0784
www.IJCSI.org

22

to improve the position estimation accuracy. The high-frequency injection method is independent of the motor model, but causes system performance degradation. Therefore, more effective rotor position estimation methods are urgently needed. Bernardes [4] researched sensorless vector control that combines two discrete-time observers to estimate the rotor speed and the position of the permanent magnet synchronous machines. Zhang [5] designed a type of magnetic levitation high speed PMSM rotor position measuring system based on fuzzy SMO. This method can suppress the chattering problem of the SMO by using the fuzzy control system, but the complex fuzzy logic makes it difficult to deploy for wider use. Guo [6] built an adaptive sliding-mode observer for back electromotive force estimation of the brushless DC motor, but this did not solve the chattering problem of the sliding mode observer and rotor position error compensation. Li [7] presented sliding mode control of the brushless DC motor based on exponential reaching law; however only simulation validation was performed. Li [8] proposed a sliding mode observer design for the brushless DC motor control system but the chattering of the sliding mode observer was still not solved by this approach. Mrashed [9] adopted a model reference adaptive method to ensure the convergence of parameter estimation, but the structure of the pure integral introduces a DC bias and an error accumulation problem. Additionally, for digital implementation, the continuous sliding mode design cannot be directly extended into the discrete domain [10]. In summary, the literature [11 12] has proposed using discrete-time sliding mode observers with direct torque control for brushless DC motors but has not solved the chattering of the sliding mode observer.

In this paper, we propose a discrete-time sliding mode observer (DSMO) for BLDCM based on exponential reaching law. This paper uses a Coordinate Rotation Digital Computer (CORDIC) [13] algorithm to obtain the rotor position and speed, since the arctan(x) usually requires a look-up table in DSP making it difficult to achieve the expected accuracy requirement. A torque loop

replaces the current loop to reduce the torque ripple of the brushless DC motors with non-ideal back-EMF.

2 The BLDCM model

It is assumed that the magnetic circuit of the BLDCM is unsaturated, regardless of the eddy current and hysteresis losses. Then its state equations of α-β static reference frame are as follows:

$$\begin{cases} di_\alpha/dt = -R/L\,i_\alpha + 1/L(u_\alpha - e_\alpha) \\ di_\beta/dt = -R/L\,i_\beta + 1/L(u_\beta - e_\beta) \\ e_\alpha = -k_e\omega\sin\theta_e \\ e_\beta = k_e\omega\cos\theta_e \end{cases} \qquad (1)$$

where i_α, i_β, u_α, u_β represent the phase current and phase voltage in the α-β static reference frame respectively, L represents the phase inductance, R is the phase resistance, Ke is the back EMF coefficient, e_α, e_β are the back electromotive forces, ω is the rotor speed and θ_e is the rotor position.

The torque expression of a brushless DC motor is as follows:

$$T_e = \frac{3}{2}(e_\alpha/\omega i_\alpha + e_\beta/\omega i_\beta)\theta_e \qquad (2)$$

Where ω is the mechanical angular velocity of the motor.

3 The design of DSMO

3.1 The improvement of reaching law.

Gao [14] proposed the discrete index asymptotic law :

$$S_{(k+1)} - S_{(k)} = -qTS_{(k)} - \varepsilon T\,\mathrm{sgn}(S_{(k)}) \qquad (3)$$

where $q>0, 1-qT>0, \varepsilon>0, T$ represents the sampling period and $Sgn(S_{(k)})$ is the sign function.

The discrete index asymptotic sampling law profoundly reveals the characteristics of sliding mode control for discrete-time system, however, it also introduces the disadvantage that the system eventually exhibits chattering near the origin, and it cannot be ensured that the system will eventually converge to the origin. Chattering is the main obstacle for discrete variable structure control system

applications, and the switching feature of Sgn function causes many chattering problems in the vector system. So we adopt the sigmoid function to replace the traditional Sgn function to improve the switching feature and weaken chattering. This effectively improves the control quality and makes the system stable and ensures it will eventually tend towards the origin. The reaching law is as follows:

$$S_{(k+1)} = (1-qT)S_{(k)} \\ -\varepsilon T(1-\exp(-|S_{(k)}|))Sigmoid(S_{(k)}) \tag{4}$$

where the Sigmoid function is just the *H* function with the following expression:

$$\begin{bmatrix} H(\tilde{i}_\alpha) \\ H(\tilde{i}_\beta) \end{bmatrix} = \begin{bmatrix} 2/[1+e^{-a(\tilde{i}_\alpha)}]-1 \\ 2/[1+e^{-a(\tilde{i}_\beta)}]-1 \end{bmatrix} \tag{5}$$

Where *a*>0 is a variable used to adjust the slope of the Sigmoid function.

3.2 The design of the current observer

Ignoring the influence of the armature reaction and considering the winding inductance to be constant, then the current equation in formula (1) can be described by:

$$i_{\alpha\beta(k+1)} = Ai_{\alpha\beta(k)} + Bu_{\alpha\beta(k)} - Be_{\alpha\beta(k)} \tag{6}$$

In equation (6) $A=I_2 e^{\phi T_s}$ and $B = I_2 \int_0^{T_s} e^{\phi \tau} \tau d\tau$, where *Ts* is the sampling period, I_2 is a two order unit matrix, and $\phi = -\frac{L}{R}$.

An observer can be built for the discrete current as:

$$\hat{i}_{\alpha\beta(k+1)} = A\hat{i}_{\alpha\beta(k)} + Bu_{\alpha\beta(k)} - B\upsilon_{\alpha\beta(k)} \tag{7}$$

Where $\hat{i}_{\alpha\beta(k)}$ is the estimated current and $\upsilon_{\alpha\beta(k)}$ is the attractive function:

$$\upsilon_{\alpha\beta(k)} = e_{\alpha\beta(k)} + J_{\alpha\beta(k)} \tag{8}$$

where the control variable $J_{\alpha\beta(k)}$ is scalar.

The sliding surfaces function can be defined by:

$$S_{\alpha\beta(k)} = \begin{bmatrix} \tilde{i}_{\alpha(k)} & \tilde{i}_{\beta(k)} \end{bmatrix}^T \tag{9}$$

where $\tilde{i}_{\alpha(k)} = \hat{i}_{\alpha(k)} - i_{\alpha(k)}$, $\tilde{i}_{\beta(k)} = \hat{i}_{\beta(k)} - i_{\beta(k)}$;

$$\tilde{i}_{\alpha(k)} = \hat{i}_{\alpha(k)} - i_{\alpha(k)}, \tilde{i}_{\beta(k)} = \hat{i}_{\beta(k)} - i_{\beta(k)}.$$

The discrete system is built as:

$$S_{\alpha\beta(k+1)} = AS_{\alpha\beta(k)} + BJ_{\alpha\beta(k)} \tag{10}$$

Substituting formula (10) into (4) gives the following equation:

$$S_{\alpha\beta(k+1)} = AS_{\alpha\beta(k)} + BJ_{\alpha\beta(k)} \\ = (1-qT)S_{(k)} \\ -\varepsilon T(1-\exp(-|S_{(k)}|)) s\, igmoid(S_{(k)}) \tag{11}$$

Therefore, the variable structure control of the discrete system is:

$$J_{\alpha\beta(k)} = B^{-1} \Big[(1-qT)S_{(k)} \\ -\varepsilon T(1-\exp(-|S_{(k)}|))Sigmoid(S_{(k)}) \\ -AS_{\alpha\beta(k)} \Big] \tag{12}$$

The discrete domain sliding mode function should satisfy the following inequality to ensure that the observer will converge:

$$(S_{i(k+1)} - S_{i(k)})Sigmoid(S_{i(k)}) < 0 \tag{13}$$

$$(S_{i(k+1)} + S_{i(k)})Sigmoid(S_{i(k)}) \geq 0 \tag{14}$$

Formula (13) ensures that the system state will be established within a finite time, and formula (14) guarantees that the system state trajectory will decrease after its first transition through the switching surface, and that the switching surface amplitude decreases through exertion.

Analysis and proof:

The improvement reaching law:

$$S_{(k+1)} = (1-qT)S_{(k)} - \\ \varepsilon T(1-\exp(-|S_{(k)}|))Sigmoid(S_{(k)}) = p \cdot S_{(k)} \tag{15}$$

IJCSI International Journal of Computer Science Issues, Volume 12, Issue 6, November 2015
ISSN (Print): 1694-0814 | ISSN (Online): 1694-0784
www.IJCSI.org

24

where $p = 1 - qT - \dfrac{\varepsilon T(1 - \exp(-|S_{(k)}|))}{|S_{(k)}|}$, obviously

$$p<1, |p| = \frac{|S_{(k+1)}|}{|S_{(k)}|}$$

(1) When $p>-1$ and $|p|<1$, $|S_{(k+1)}| < |S_{(k+1)}|$, $|S_{(k)}|$ will decrease

(2) When $p<-1$ and $|p|>1$, $|S_{(k+1)}| > |S_{(k+1)}|$, $|S_{(k)}|$ will increase

(3) When $p=-1$ and $|p|=1$, $|S_{(k+1)}| = |S_{(k+1)}|$, $|S_{(k)}|$ will enter the chattering state

According to reaching law, parameter ε has the greatest effect and the chattering can be reduced by decreasing ε. However, if ε is too small, the switching speeds at the switching surfaces will be influenced. The sampling period T cannot be very small due to limitations of technology and equipment, etc. Thus, ideally, ε should be time-varying.

From the above analysis of the chattering, it can be determined that $S_{(k)}$ will decrease only when $p>-1$,

If it is considered that $\varepsilon = |S_{(k)}|$, then

$$p = 1 - qT - \frac{\varepsilon T(1 - \exp(-|S_{(k)}|))}{|S_{(k)}|} > -1 \qquad (16)$$

and then:

$$T < \frac{2}{q + 1 - \exp(-|S_{(k)}|)} \qquad (17)$$

$|S_{(k)}|$ is decreased if the sampling time

$T < \dfrac{2}{q + 1 - \exp(-|S_{(k)}|)}$. The reaching condition is then:

$$\begin{aligned} &(S_{i(k+1)} - S_{i(k)}) Sigmoid(S_{i(k)}) \\ &= -qT|S_{(k)}| - |S_{(k)}| \cdot (1 - \exp(-|S_{(k)}|)) \cdot T < 0 \end{aligned} \qquad (18)$$

$$\begin{aligned} &(S_{i(k+1)} + S_{i(k)}) Sigmoid(S_{i(k)}) \\ &= (2 - qT)|S_{(k)}| - |S_{(k)}|(1 - \exp(-|S_{(k)}|)) \cdot T \\ &= \left[(2 - qT) - (1 - \exp(-|S_{(k)}|)) \cdot T \right] \cdot |S_{(k)}| \geq 0 \end{aligned} \qquad (19)$$

Thus, the system satisfies the reaching condition of sliding mode.

3.3 The design of the EMF observer

The back EMF observer is built to extract the back EMF signal directly, in order to improve the estimation precision of the rotor position. The low pass filter is also eliminated, as its phase delay reduces the rotor position estimation accuracy.

The dynamic characteristics of the back electromotive force in formula (1) are taken to perform the discretization.

$$e_{\alpha\beta(k+1)} = e_{\alpha\beta(k)} + T_s \omega_{e(k+1)} L e_{\alpha\beta(k)} \qquad (20)$$

Where $\omega_{e(k)}$ slowing changes over two consecutive sampling cycles, $\Delta\omega_{e(k)} \approx 0$, $L = \begin{bmatrix} 0 & -1 \\ 1 & 0 \end{bmatrix}$.

The self-adapting back EMF observer is built as:

$$\hat{e}_{\alpha\beta(k+1)} = \hat{e}_{\alpha\beta(k)} + T_s \hat{\omega}_{e(k+1)} L e_{\alpha\beta(k)} - h_3 \tilde{e}_{\alpha\beta(k)} \qquad (21)$$

where h_3 and $\hat{\omega}_{e(k+1)}$ represent the constant and estimated rotor speed respectively, the estimated error of the back electromotive force is $\tilde{e}_{\alpha\beta(k)} = \hat{e}_{\alpha\beta(k)} - e_{\alpha\beta(k)}$, and the estimated error of the subsequent speed can be found using the self-adaption law as:

$$\tilde{\omega}_{e(k+1)} = \frac{\tilde{\omega}_{e(k)}}{1 + \frac{T_s^2}{2}\gamma \| e_{\alpha\beta(k)} \|_2^2} - \frac{T_s\gamma(1 - h_3)(\tilde{e}_{\alpha\beta(k)}^T L e_{\alpha\beta(k)})}{1 + \frac{T_s^2}{2}\gamma \| e_{\alpha\beta(k)} \|_2^2} \qquad (22)$$

where γ represents a positive constant. Thus, if $h_3 \in (0,2)$, then the estimated back electromotive force $\hat{e}_{\alpha\beta(k)}$ and rotor speed $\hat{\omega}_{e(k)}$ converge to their actual values $e_{\alpha\beta(k)}$ and $\omega_{e(k)}$.

IJCSI International Journal of Computer Science Issues, Volume 12, Issue 6, November 2015
ISSN (Print): 1694-0814 | ISSN (Online): 1694-0784
www.IJCSI.org

25

From formula (20) and (21), the value of the estimated back electromotive force can be obtained as:

$$\tilde{e}_{\alpha\beta(k+1)} = (1-h_3)\tilde{e}_{\alpha\beta(k)} + T_s \tilde{\omega}_{e(k+1)} L e_{\alpha\beta(k)} \qquad (23)$$

where $\tilde{\omega}_{e(k)} = \hat{\omega}_{e(k)} - \omega_{e(k)}$ is the estimated error, and the Lyapunov function is selected as:

$$V_{(k)} = \tilde{e}_{\alpha\beta(k)}^T \tilde{e}_{\alpha\beta(k)} + \gamma^{-1} \tilde{w}_{e(k)}^2 \qquad (24)$$

where γ is a positive constant.

The error of the Lyapunov function is:

$$\Delta V_{(k)} = \tilde{e}_{\alpha\beta(k+1)}^T \tilde{e}_{\alpha\beta(k+1)} \\ - \tilde{e}_{\alpha\beta(k)}^T \tilde{e}_{\alpha\beta(k)} + \gamma^{-1}(\tilde{\omega}_{e(k+1)}^2 - \tilde{\omega}_{e(k)}^2) \qquad (25)$$

In order to ensure the stability of the back EMF observer, the value of $\triangle V_{(k)}$ in formula (25) must be a non-positive number.

Substituting formula (22) and (23) into (25) gives:

$$\Delta V_{(k)} = [(1-h_3)^2 - 1] \| \tilde{e}_{\alpha\beta(k)} \|_2^2 - \gamma^{-1}\Delta\tilde{\omega}_{e(k)}^2 \qquad (26)$$

If $h_3 \in (0,2)$, then $\Delta V_{(k)}$ has a negative value so $\tilde{e}_{\alpha\beta(k)}$、$\tilde{\omega}_{e(k)}$ and formula (26) converge to zero, and the slider observer is stable. This further shows that the stability of the rotor position and speed estimation are only related to h_3 and changes in the parameters of the motor will not affect the stability of the observer.

Using the observed value of the back electromotive force, the rotor position can be estimated as:

$$\hat{\theta}_{e(k+1)} = \tan^{-1}(-\hat{e}_{\alpha(k+1)} / \hat{e}_{\beta(k+1)}) \qquad (27)$$

3.4 The design of CORDIC

The CORDIC [15] processor is an iterative computation and its system configuration block diagram is shown in Fig.1

If $Z_0 = 0$, then $X_N \to \dfrac{1}{0.6072}\sqrt{X_0^2 + Y_0^2}$,

and $Y_N \to 0$, $Z_N \to \arctan(\dfrac{Y_0}{X_0})$. Additionally, in order to ensure that the angle meets the criteria $\theta \in (0, 2\pi)$, the participating angle should undergo both pre-treatment and post-treatment.
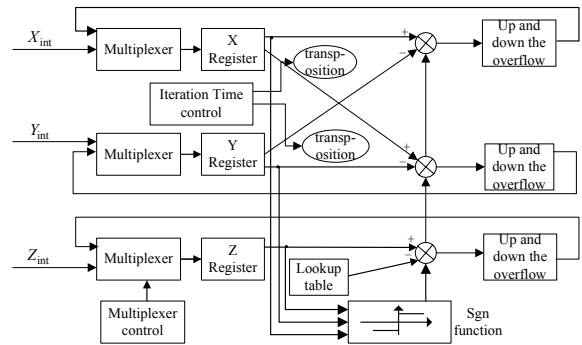

Fig. 1: Block diagram of CORDIC processor

4 Simulation and experiment

The structure diagram of the discrete-time sliding mode observer (DSMO) for BLDCM based on the exponential reaching law is shown in Fig.2
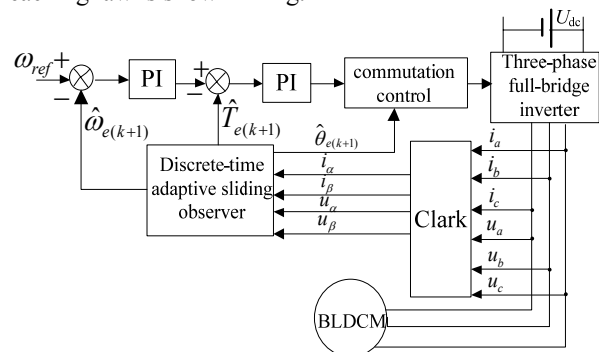

Fig. 2: Structure diagram of BLDCM sensorless control

4.1 Simulation

Tab.1: Parameters of the motor for simulation

Parameter	Value
Rated Voltage U_N	24V
Rotor Torque T_N	2.1 N·m
Rotor Speed n_N	3000 r/min
Phase Resistance R	0.66Ω
Effective Inductance	1.442 H
Potential Coefficient K_e	0.067 V/(rad/s)
Rotational Inertia J	1.57×10^{-5} kg·m²

IJCSI International Journal of Computer Science Issues, Volume 12, Issue 6, November 2015
ISSN (Print): 1694-0814 | ISSN (Online): 1694-0784
www.IJCSI.org

26

The simulation is performed using Matlab/Simulink to validate the proposed control method. The traditional sliding mode observer (TSMO) and the discrete-time sliding mode observer (DSMO) are both used to control BLDCM. Table 1 gives the main parameters of the motor used.

Figure 3 and 5 display the rotor speed using TSMO and DSMO respectively, and Figure 4 and 6 are the corresponding enlarged graphs of the rotor speed.
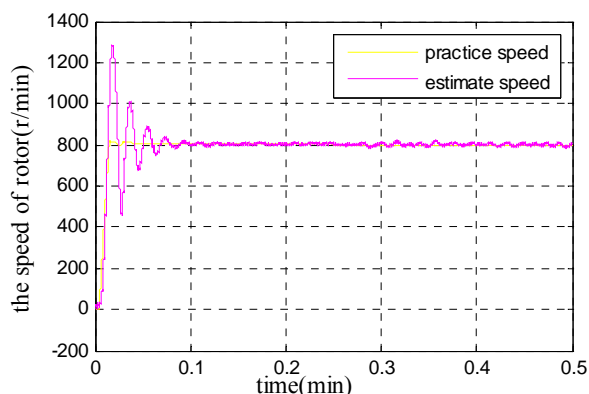
Fig. 3: Speed diagram of TSMO
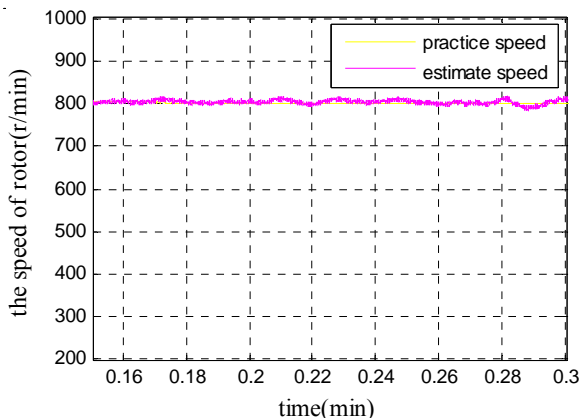
Fig. 4: partially enlarged speed diagram of TSMO
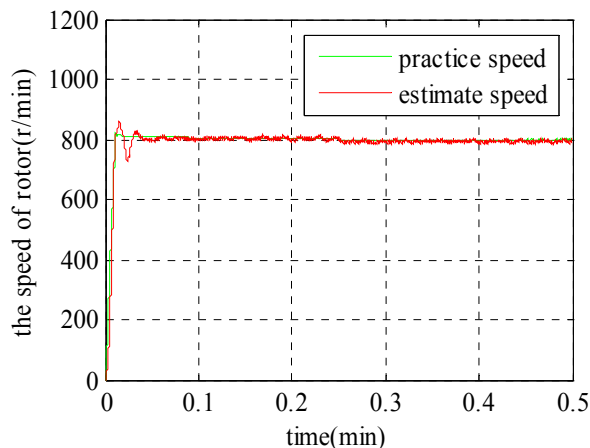
Fig. 5: Speed diagram of DSMO
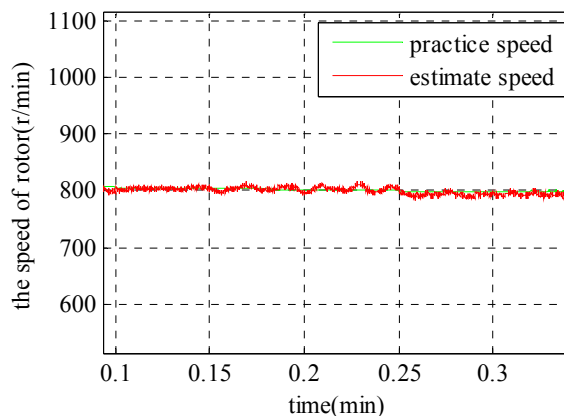
Fig. 6: partially enlarged speed diagram of ISMO

From Figure 3, 4, 5 and 6, the overshoot with the TSMO is found to be 52% and it can be observed that the estimated speed chatters heavily. However, the overshoot is just 12% with the DSMO and the estimated speed is relatively stable and tracks the actual speed. Both TSMO and DSMO control have strong anti-load-disturbance ability.

Figure 7 and 8 are the rotor position diagrams with TSMO and DSMO. The initial speed of the rotor is 800r/min, which is increased to 1500 r/min at 0.3min and an additional load of 1N·m is added at 0.6min. Figure 9 shows the average absolute values of the rotor position error under different speeds and different control strategies.

IJCSI International Journal of Computer Science Issues, Volume 12, Issue 6, November 2015
ISSN (Print): 1694-0814 | ISSN (Online): 1694-0784
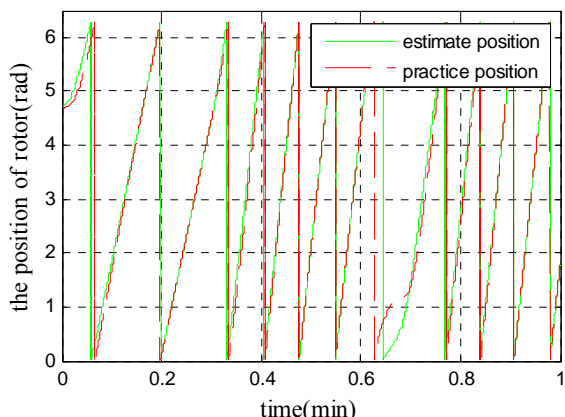www.IJCSI.org

27
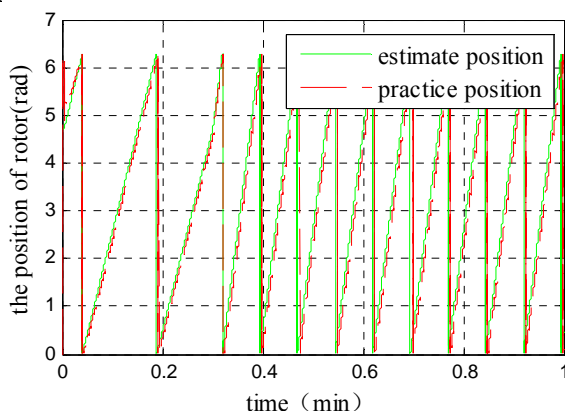
Fig. 7: Rotor position diagram of TSMO
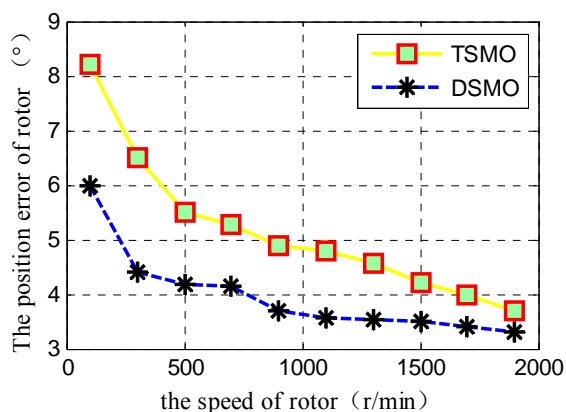

Fig. 8: Rotor position diagram of DSMO

Fig. 9: Waveform of BLDCM rotor position error

From Figure 7, 8 and 9, it can be observed that when the rotor speed is 800r/min under TSMO and DSMO, the average absolute values of the rotor position error are 5° and 3.9°. At 0.3min when the rotor speed is 1500r/min, the errors are respectively 4.2° and 3.7°. At 0.6min when an additional load of 1N·m is added, the DSMO control has a stronger ability to resist load disturbance and reduce flutter, as shown in Figure 7 and 8. The position error of the rotor also decreases as the speed increases, further verifying the rationality of the proposed method.

4.2 Experiment

The master control board consists of a DSP-TMS320F28335 and a FPGA-EP2C35F484C8N. The experimental platform of the discrete-time sliding mode observer (DSMO) for BLDCM based on exponential reaching law is shown in Figure 10. The motor parameters are the same as those used in the simulation.
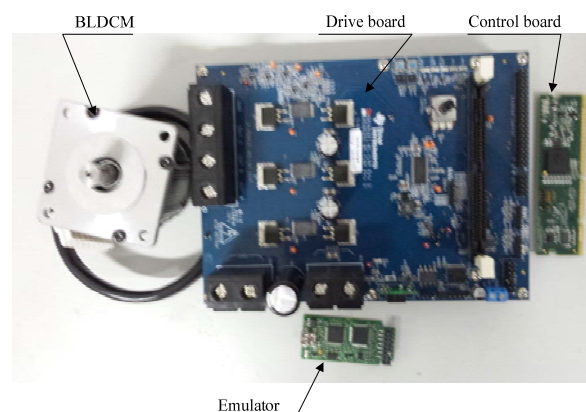

Fig. 10: Experimental platform

Figure 11 and 12 are the rotor position diagrams using TSMO and DSMO when the rotor speed is 800r/min. Figure 13 shows the average absolute values of the rotor position errors under different speeds.
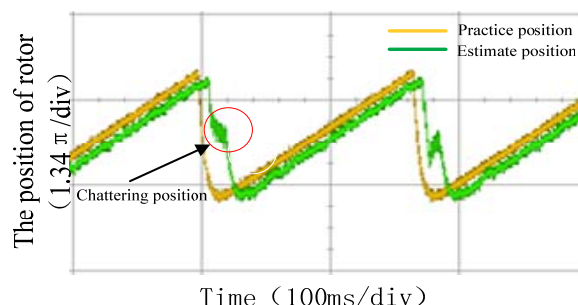

Fig. 11: Rotor position diagram of TSMO
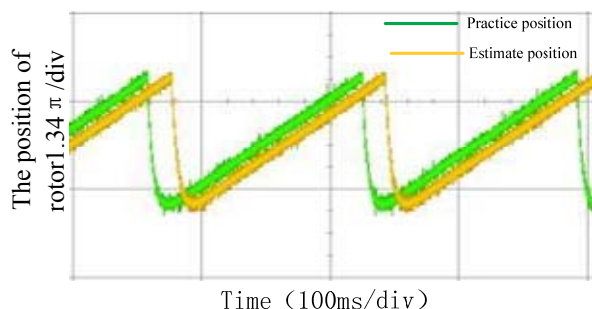
IJCSI
www.IJCSI.org
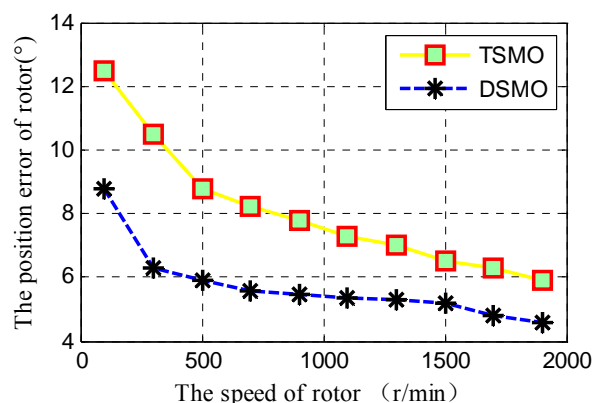
Fig. 12: Rotor position diagram of ISMO

Fig. 13: Waveform of BLDCM rotor position error

From Figure 11, 12 and 13, we can observe that when the rotor speed is 800r/min under TSMO and DSMO, the average absolute values of the rotor position errors are 7.8° and 5.5°. Experiments verify the result of the simulation and also verify the rationality of the method proposed in this paper.

5 Conclusions

Using the theory of discrete sliding mode, we propose a discrete-time sliding mode observer (DSMO) for BLDCM based on the exponential reaching law. The rotor position and speed are estimated, and the sigmoid function is used with the sliding-mode control to significantly weaken chattering which occurs in sliding mode. The back EMF observer is built to extract the back EMF signal directly, eliminating the low pass filter and phase angle compensation. The CORDIC algorithm is introduced to precisely estimate rotor position. The results from simulation and experiments both show that the new sliding mode controller can significantly weaken chattering, accurately estimate the rotor position and provide good dynamic and static stability.

Acknowledgments

References

[1] Xia C.L . The contool system of BLDC motor[M]．Beijing:Science Press,2009:1-12.

[2] Zou J.B, Jiang S.L,Zhang H.L. A novel method of detecting for rotor position of a sensorless brushless DC motor [J]. Transactions of China Electrotechnical Society, 24(4), 2009, 48-53.

[3] Y. Inoue, Y. Kawaguchi, S. Morimoto, and M. Sanada. Performance improvement of senseless IPMSM drives in a low-speed region using online parameter identification [C], IEEE Trans. Ind. Appl, 47(2) , 2011, 798–804.

[4] B.Thiago, F. M. Vinícius, A.G. Hilton, and Humberto Pinheiro. Discrete-Time Sliding Mode Observer for Sensorless Vector Control of Permanent Magnet Synchronous Machine[J], IEEE Transactions on Industrial Electronics, 61(4), 2014,1679-1691.

[5] Zhang H.S,et al, Rotor Position Measuring Method for Magnetic Levitation High Speed PMSM Based on Fuzzy Sliding Mode Observer[J], Transactions of China Electrotechnical Society,29(7),2014,147-153.

[6] Guo H.H, Zhou B, Zuo G.J, et al. Adaptive sliding-mode observer for back electromotive force estimation of brushless DC motor [J]. Proceedings of the CSEE, 2011, 31(21): 142-149.

IJCSI
www.IJCSI.org

IJCSI International Journal of Computer Science Issues, Volume 12, Issue 6, November 2015
ISSN (Print): 1694-0814 | ISSN (Online): 1694-0784
www.IJCSI.org

29

[7] Zhang Y.D, Zhang M.sliding mode control of brushless DC motor with exponential reaching law[J],Motor and control application , 2011,38(3):32-35.

[8] Li X.X, Zhu Z.F, Zhao H.M. BLDCM without position control system design based on the sliding mode observer [J].Journal of circuits and system, 2009,14(2):79-83.

[9] Mrashed, C. PFA Mac, S.AF, A. P. Senseless Indirect rotor Field Orientation Speed Control of Permanent Magnet Synchronous Motor Using Adaptive rotor Flux Estimator[J].IEEE Control Conference and the European Control Conference ,15(10),2005 ,647-652.

[10] R.P.Vieira, C.C.Gastaldini, et al, Discrete-time sliding mode speed observer for senseless control of induction motor derives [J]. IET Electric Power Applications, 2012, 6(9):681-688.

[11] Zhao Y, Yang Y.J, Zhang W. Discrete-time sliding mode observers on direct torque control for brushless DC motor, ELECTRIC DRIVE, 2012, 42(5), 16-19.

[12] B.Thiago, F. M. Vinícius, A.G. Hilton, and Humberto Pinheiro. Discrete-Time Sliding Mode Observer for Sensorless Vector Control of Permanent Magnet Synchronous Machine[J], IEEE Transactions on Industrial Electronics, 61(4), 2014,1679-1691.

[13] Yang Y, Tang X.C, Deng S.C. Application of CORDIC Algorithm in Resolver-to-digital and PMSM Vector-control Based on FPGA, MICROMOTORS, 2013, 46(7):68-73.

[14] Gao W.B. variable structure control of discrete time system[J], Acta Automatic Sinica, 1995,20（2）:154-161.

[15] Zhang D.Z, Zhang S.B, et al, Application of CORDIC in Capacitive Rotary Encoder Signal Demodulation [J], 2012 the 8th IEEE International Symposium on Instrumentation and Control Technology, 2012:61-65.